Theoretical comparison of multiple quantum wells and thick-layer designs in InGaN/GaN solar cells

Nicolas Cavassilas, Fabienne Michelini, Marc Bescond

Theoretical comparison of multiple quantum wells and thick-layer designs in InGaN/GaN solar cells

Nicolas Cavassilas, Fabienne Michelini, Marc Bescond
IM2NP, UMR CNRS 7334, Aix-Marseille Université, 13384 Marseille, France

This theoretical work analyzes the photovoltaic effect in non-polar InGaN/GaN solar cells. Our electronic transport model considers quantum behaviors related to confinement, tunneling, electron-phonon and electron-photon scatterings. Based on this model we compare a multiple quantum wells cell with its thick-layer counterpart. We show that the structure of multiple quantum wells is a promising design providing better compromise between photon-absorption and electronic transport. This balance is necessary since these two phenomena are shown to be antagonist in nanostructure based solar cells. In this type of devices we also show that phonon absorption increases the short-circuit current while phonon emission reduces the open-circuit voltage.

PACS numbers: Valid PACS appear here

InGaN alloys have been extensively used to make light-emitting diodes and laser diodes with a large range of emission wavelengths. More recently, InGaN alloys have also received attention for photovoltaic applications. This interest is particularly motivated by the direct band gap (E_G) of these materials ranging from 0.64 eV for InN to 3.4 eV for GaN. This characteristic is found to be even more interesting for multijunction solar cells. The actual record of 44.7% for a photovoltaic cell has been achieved by a multijunction device with four subcells [1]. To go beyond this success it may be necessary to increase the number of junctions. For a five-subcell device, the top material ideally requires a bandgap of 2.5-2.6 eV [2]. This indicates the tremendous potential of InGaN-based alloys with band gaps greater than 2.2 eV for which few alternative materials currently exist [3, 4].

In that context InGaN/GaN photovoltaic devices have been the subject of many studies. On C-plane substrate multiple quantum well (MQW) devices [3, 4] show better performances than the quasi-bulk double heterojunction devices [5, 6]. This result could be explained by a high density of dislocations in thick-layer due to the lattice mismatch between the layer and the substrate. In contrast the synthesis of nanowires can be virtually substrate-free, which prevents the formation of dislocations [7]. Moreover this approach permits to have non-polar heterojunctions unlike conventional C-plane structures where internal polarization fields reduce the quantum efficiency [8].

To advance the development of InGaN photovoltaic technology it is now necessary to better analyze the physical behavior of these devices based on sophisticated quantum simulations. This behavior is complex because it depends on several physical phenomena that are generally tackled separately such as quantum confinement, photon absorption, tunneling, electron-phonon scattering, drift-diffusion. However, in the considered nanostructured devices, these phenomena become interdependent. It is therefore necessary to assume a global quantum transport model. In this work we use the non equilibrium green functions (NEGF) formalism to model the electronic quantum transport with interactions [9]. In a nanoscale device we can calculate the current of electrons and holes generated by a given power spectrum of light [10, 11]. Although a large number of approximations are necessarily assumed, this model gives a clear overview of the physical behavior of the solar cell.

In this article, we compare a MQW with a thick-layer structure and focus on non-polar heterojunctions [8]. We calculate and analyze $I-V$ characteristics, current spectra and local density of states (LDOS). Our results show that the MQW structure offers a better quantum efficiency due to a better compromise between photon-absorption and electronic-transport. We also analyze the electron-phonon scattering induced effect.

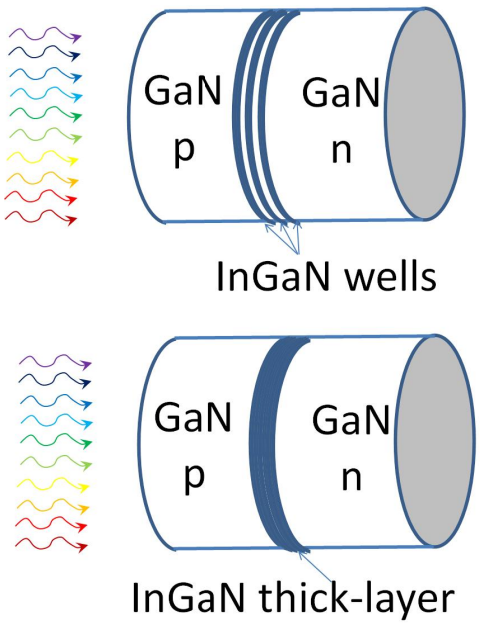

FIG. 1. Schematic representation of the two considered solar cells. (N_A=5 10^{23} m^{-3}, N_D=10^{24} m^{-3}, L$_n$=40 nm, L$_p$=80 nm).

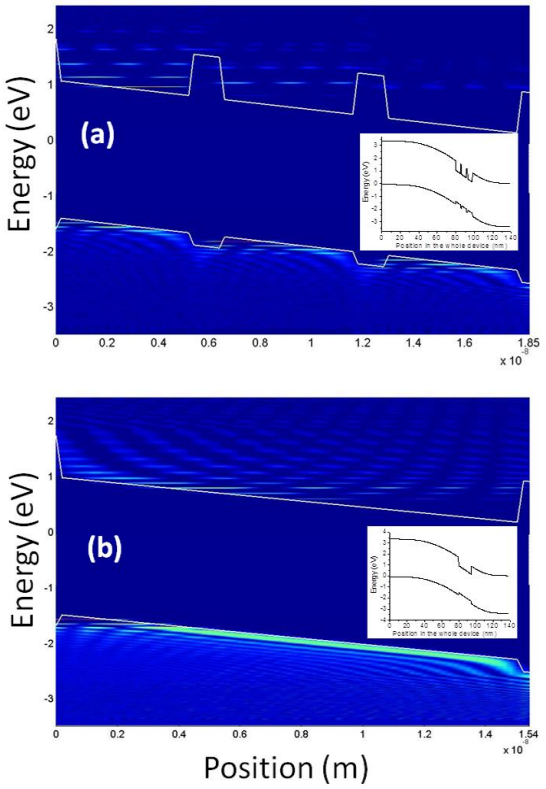

FIG. 2. LDOS in active region of (a) the MQW and (b) the thick-layer solar cells. Inset: band diagram in the whole device. Electron-phonon scattering is included. V=0 V.

The two considered devices are schematically represented Fig. 1. The MQW device is defined by three 5 nm quantum wells of $In_{0.25}Ga_{0.75}N$ (E_G=2.46 eV) separated by 1 nm GaN barriers while the thick-layer device has simply an active region of 15 nm of $In_{0.25}Ga_{0.75}N$. In both solar cells the active regions are embedded in doped GaN. In MQW solar cell we have chosen very thin GaN barriers to obtain a strong tunneling. Photocurrent is then expected to be large [13] which facilitates the numerical implementation of the model. Indeed, a weak tunneling coupling would generates very localized quantum well states with narrow spectral functions. It would be then necessary to have a very fine energy mesh in the model.

We assume a potential invariance in the transverse plan permitting to separate the 2D dispersion from the 1D transport. The 1D quantum transport model is based on the NEGF formalism in which the solar cell is connected to two semi-infinite reservoirs. The dispersion relation of electron is defined by a two-band (conduction and valence bands) effective mass Hamiltonian. These two bands are only coupled *via* interactions with light. Band-to-band tunneling, excitonic effect and intraband radiative transitions are ignored. Electrostatic potential along the transport axis is self-consistently calculated using the Poisson's equation. considering the majority carriers only with a energy step of 5 meV. Scatterings are described within the self-consistent Born approximation [14] only in the intrinsic active region of the device with an energy step of 1 meV. Due to important numerical burden, electron-phonon scattering is only included in part of the calculations through polar optical phonon interactions. Photon incident flux is assumed to propagate along the electronic transport direction with a spectra profile of the black-body at 6000 K. For further details on our model see Ref. [11].

The band diagram and LDOS are shown Fig. 2 for the two solar cells. We first see that the band discontinuities induce peaked densities of states in both devices. In MQW many states of the conduction band are localized in quantum wells. Electrons generated on these states can reach reservoirs by tunneling and/or by electron-phonon scattering. We also show states directly connected to reservoir *i.e.* above the GaN barriers. Because these barriers still generate reflection for high kinetic energy electrons, the corresponding states are quasi-localized. It is worth noticing that the better the state is connected to reservoirs (directly, by scattering or by tunneling), the more important is its broadening. This broadening has an impact on light absorption while it is related to electronic transport. This is an example of the

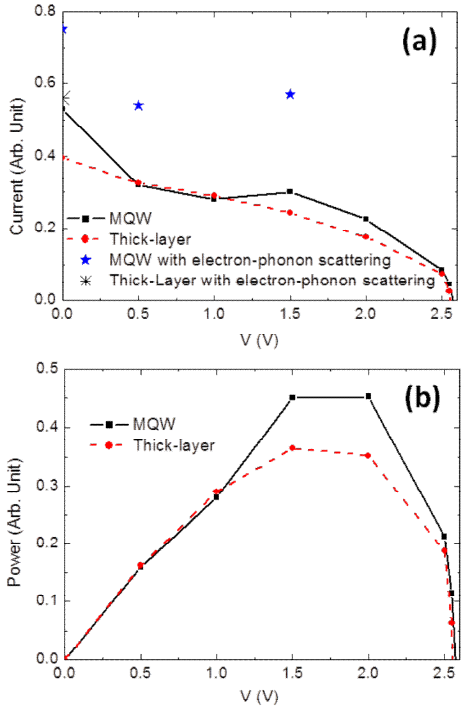

FIG. 3. (a) Current characteristics for the two considered devices (MQW and thick-layer) obtained without phonon interactions and also some points obtained with electron-phonon scattering. (b) Power characteristics for the two considered devices obtained without phonon interactions.

interdependance of phenomena occurring in photovoltaic devices [12].

In the thick-layer device shown Fig. 2(b), most of states are directly contacted to reservoirs. However these delocalized states might absorb less photons since LDOS peaks in conduction and valence bands can be spatially remote (*i.e.* with a weak overlap). So in this nanostructured devices, promoting transport properties can reduce photon absorption, and *vice versa*. The best performance will be therefore obtained for a good compromise.

Figure 3 shows the illuminated current (I) and power (P) characteristics for both devices. We first see that, without phonon, current and power are slightly larger in the MQW than in the thick-layer. Compromise between absorption and transport is therefore better in the case of MQW. More precisely the short circuit current I_{sc} is higher in MQW (0.53 *versus* 0.39 a.u.) while the open circuit voltages V_{oc} are similar (2.6 V). In both cases the photocurrent is very dependent on electric field and we observe low fill-factors (0.33 and 0.35 for the MQW and the thick-layer respectively). Indeed, increase of V enlarged the triangular GaN tunneling barriers (at right for electrons and at left for holes). It then becomes increasingly difficult for carriers generated in the active region to reach reservoirs and to contribute to the current. Figure 3 also shows that characteristic for MQW is nonmonotonic and that incorporation of electron-phonon scattering increases the current for both cells. These original behaviors are explained in the following by current spectra and LDOS analysis.

Figure 4 shows current spectra calculated with electron-phonon scattering at V=0 V in both structures. MQW has less peaks than the thick-layer cell but their intensity is larger. The localized states provide a better quantum efficiency although carriers must then escape by tunneling and/or scattering. We deduce that localized states absorb many photons. Unfortunately a lot of states in quantum well absorb photons but do not generate current because they are too localized. How efficiently increase the number of useful localized states may be the subject of future design optimizations.

If tunneling is of prime importance in MQW, Fig. 4(b) shows that it has also an impact in the thick-layer device. Indeed, the most intense peaks of current are related to tunneling across the triangular GaN barriers located at the edges of the active region. These peaks correspond to the absorption of low-energy photons which are more numerous and for which the conduction-valence coupling is stronger.

Figure 5 shows the LDOS in MQW for the local current maximum obtained at V=1.5 V in Fig. 3. At that bias, several localized states are aligned inducing a strong resonant tunneling and also a level broadening of the corresponding LDOS peaks. This bias-dependent alignment tends to increase the current and it is at the origin of the nonmonotonic feature of the $I-V$ characteristic. More generally, it can be expected that a cell with a few wells will exhibit a nonmonotonic current characteristic.

In these devices electron-phonon scattering have two opposite impacts. This scattering can assist tunneling [15] and phonon absorption are responsible for thermionic emission [13]. This explains the larger I_{sc} with phonon interactions shown Fig. 3 for both devices. On the other hand, electron-phonon scattering also promotes electron-hole recombination. Carriers may reach the very localized ground states of quantum wells by phonon emission and recombine by photon emission. This effect induces localized negative current contributions as shown Fig. 6 (current spectra for V=1.5 V in MQW). The expected consequence of this behavior is a reduction of V_{oc}. Unfortunately, this could not be verified in this work because when this effect concerns the majority carriers at large bias, it becomes strong and it is very difficult to converge the self-consistent Born loop [14].

In conclusion our results confirm that MQW is a promising candidate for photovoltaic applications. Indeed, even without dislocation, we obtained a larger generated power in MQW cell than in its thick-layer counterpart. More generally this study sheds light on the photovoltaic effect in nanostructure based devices. We show that localized states absorb many photons while free electron states provide good transport properties. However, such transport behaviors like tunneling, assisted phonon tunneling, thermionic emission and resonant tunneling

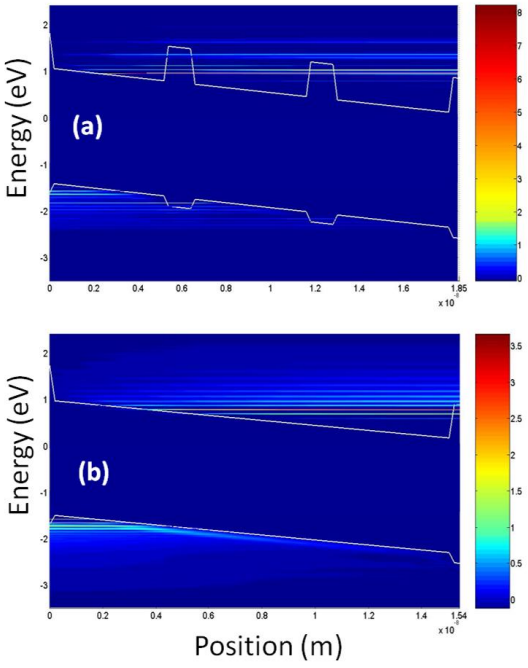

FIG. 4. Current spectra (in arbitrary unit) in the active region for (a) the MQW and (b) the thick-layer solar cell. Electron-phonon scattering is included. V=0 V.

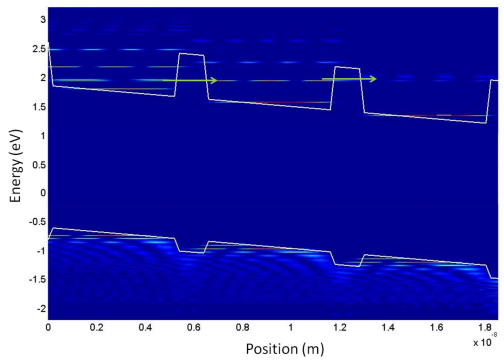

FIG. 5. LDOS in the active region of the MQW solar cell. The green arrows represent the strong tunneling due to alignment of localized states in quantum wells. Electron-phonon scattering is included. V=1.5V.

can provide a excellent quantum efficiency to localized states. But this efficiency, since it is highly dependent on confinement and bias, is precarious and strongly localized states do not generate current. Future studies should propose solutions to increase the number of efficient localized states. Finally simulations show the two opposite impacts of electron-phonon scattering while facilitating the escape from localized states, increases electron-hole radiative recombination. Consequently I_{sc} is increased while V_{oc} is expected to be reduced.

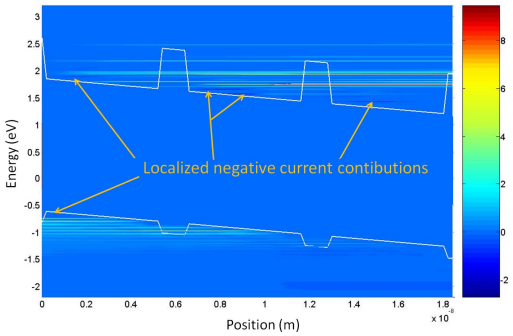

FIG. 6. Current spectra (in arbitrary unit) in the active region for the MQW solar cell. Electron-phonon scattering is included. V=1.5 V.

[1] http://phys.org/news/2013-09-world-solar-cell-efficiency.html

[2] Nikholas G. Toledo, Daniel J. Friedman, Robert M. Farrell, Emmett E. Perl, Chieh-Ting (Tony) Lin, John E. Bowers, James S. Speck and Umesh K. Mishra J. Appl. Phys. 111 , 054503 (2012)

[3] R. M. Farrell, C. J. Neufeld, S. C. Cruz, J. R. Lang, M. Iza, S. Keller, S. Nakamura, S. P. DenBaars, U. K. Mishra and J. S. Speck, Appl. Phys. Lett. **98**, 201107 (2011).

[4] N. G. Young, R. M. Farrell, Y. L. Hu, Y. Terao, M. Iza, S. Keller, S. P. DenBaars, S. Nakamura and J. S. Speck, Appl. Phys. Lett. **103**, 173903 (2013).

[5] Carl J. Neufeld, Nikholas G. Toledo, Samantha C. Cruz, Michael Iza, Steven P. DenBaars and Umesh K. Mishra, Appl. Phys. Lett. **93**, 143502 (2008).

[6] J. R. Lang, C. J. Neufeld, C. A. Hurni, S. C. Cruz, E. Matioli, U. K. Mishra and J. S. Speck, Appl. Phys. Lett. **98**, 131115 (2011).

[7] Yajie Dong, Bozhi Tian, Thomas J. Kempa and Charles M. Lieber, Nano Lett. **9**, 2183 (2009).

[8] Yue Jun Sun, Oliver Brandt, Sven Cronenberg, Subhabrata Dhar, Holger T. Grahn, Klaus H. Ploog, Patrick Waltereit, and James S. Speck, Phys. Rev. B **67**, 041306(R) (2003)

[9] W. Meir and N. S. Wingreen, Phys. Rev. Lett. **68**, 2512 (1992).

[10] U. Aeberhard, J. Comput. Electron. **10**, 394 (2011).

[11] N. Cavassilas, F. Michelini and M. Bescond, J. Renewable Sustainable Energy **6**, 011203 (2014).

[12] A. Berbezier, J.-L. Autran and F. Michelini, Appl. Phys. Lett. **103**, 041113 (2013).

[13] J. R. Lang, N. G. Young, R. M. Farrell, Y.-R. Wu and J. S. Speck, Appl. Phys. Lett. **101** , 181105 (2012).

[14] N. Cavassilas, M. Bescond, H. Mera, and M. Lannoo, Appl. Phys. Lett. **102**, 013508 (2013).

[15] V. J. Goldman, D. C. Tsui, and J. E. Cunningham, Phys. Rev. B **36**, 7635 (1987).